CHAPTER 190

DYNAMIC RESPONSE OF VERTICAL ELASTIC WALLS TO BREAKING WAVE IMPACT

Masatato Hattori[1] and Nobuaki Tsujioka[2]

Abstract

Experiments were focused on deflection responses of the wall member of upright structures to impulsive wave forces. The experiments revealed that the wall deflection response depends on wave loading modes as well as on natural frequency of the wall member system, f_{NW}. Single degree-of-freedom model of transient impact shows that the peak wall deflection is given as a function of the ratio between rise time of wave force τ_F and f_{NW}, representing characteristics of the wave load and the wall member. The measured peak deflection agrees well with the predicted by the model. In addition, the model indicates that with decreasing natural frequencies of the wall system, the wave load mode brought about greater peak deflections changes from the mode of short duration force to that of long-lasting force.

Introduction

Steep breaking waves impinging onto upright structures bring about high impact forces of short duration. It has been considered that such impact forces are not the cause of sliding and/or overturning of massive structures. On the other hand, some studies (e.g., Weggel and Maxwell, 1970; Mogridge and Jamieson, 1980) pointed out a possibility that the impact force will cause a cumulative and local damage due to shear and fatigue failures to the structure. As a result of successive attacks of the breaking wave, such damage grows likely into a sudden breakdown of the structure.

---

1 Professor, Department of Civil Engineering, Chuo University, Bunkyo-ku, Tokyo 112, Japan.
2 Graduate-Student, ditto.

The failure processes, therefore, seem to be relevant to deflection responses of the wall member to the impact.

Many studies have been conducted to provide functional information on the stability of upright structures. In contrast with this, as far as we know, only three previous studies (Witte, 1988; Kirkgöz, 1990; Hattori, 1994) have discussed dynamic responses of the vertical wall to impact wave pressures. Therefore, more precise studies are requested to deepen our understanding of the deflection response of elastic walls, as the first step toward the explication of failure processes of the wall member.

Accordingly, we conducted a series of comprehensive experiments with the following objectives;

(1) to build up the reliable data base of deflection responses of the vertical wall due to impulsive wave forces for designing the structures,

(2) to examine influences of the wave loading mode and the physical property of elastic walls on the wall deflection response, and

(3) to discuss a critical condition, producing the greatest wall deflection, based on a single degree-of-freedom model of transient impact.

Experimental setup and Measurements

Figure 1 shows the general arrangement of experimental setup. Experiments were conducted in a glass-walled wave flume, 0.30 m wide, 0.55 m high, and 20 m long, in which a steel plane beach of 1/20 slope was installed. Regular waves were produced by a reflection-absorbing wave maker of flap-type, controlled by a programmed analogue signal yielding a regular wave train. Vertical wall complex was mounted rigidly on a plastic mound with a foreshore slope of 1/10. Except for the wall complex, the experimental setup and measuring techniques used in this study are basically the same as those used in the previous study (Hattori et al. 1994).

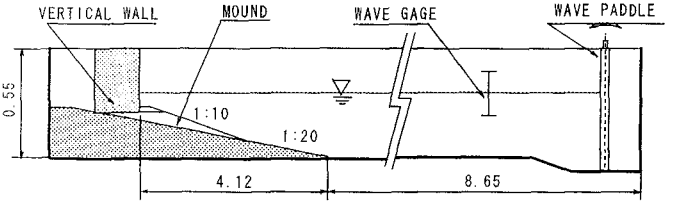

Fig. 1 General arrangement of the experimental setup. (units: m)

Vertical wall is composed of two parts, the rigid wall of 10 mm-thick steel plate (0.30 m wide and 0.50 m high) and the square elastic wall as shown in Fig. 2. The elastic wall is a thin plate fully fixed each side with rigid steel frames, and it is

inlaid into the lower section of the rigid wall. Taking into account influences of the wall physical property on the deflection response, we used three elastic plates with different properties (Table 1).

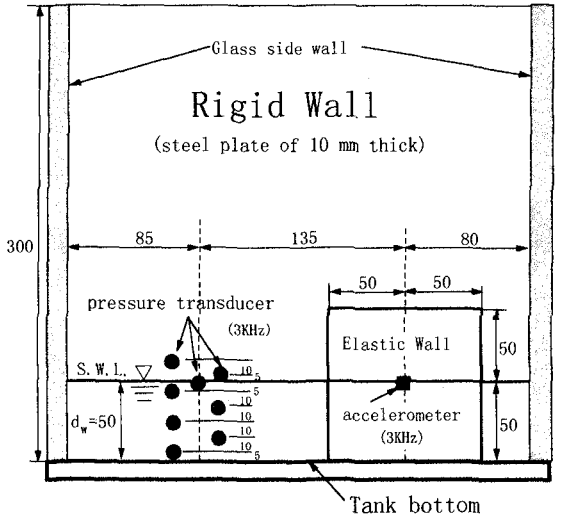

Fig. 2 Wave tank cross-section showing the location of rigid and elastic walls. (units: mm)

Table 1 Physical properties of the elastic plates.

Plate	Thickness (mm)	Density (g/cm^2)	E (KN/m^2)	f_{NW} (Hz)	
				in air	in water
Spring metal	1.0	9.0	1.0×10^8	557	271
	0.5	9.0	1.0×10^8	290	100
Polyvinyl chloride	0.5	1.14	1.6×10^7	300	59

E: Modulus of elasticity.

In this study, the wall deflection response will be examined in terms of the natural frequency of the elastic wall system, f_{NW}, as a relevant parameter representing dynamic characteristics of the elastic wall. Taking account of added mass effect of ambient water in front of the wall, the natural frequency (first mode) of wall deflection system (abbreviated to W-D system) were calibrated by a pendulum test with changing the water depth in front of the wall. As an example, the natural

frequency of 1 mm-thick spring metal plate wall is given by Fig. 3, as a function of the relative water depth d_w/h_a (d_w: water depth at the wall, and h_a: elastic wall height).

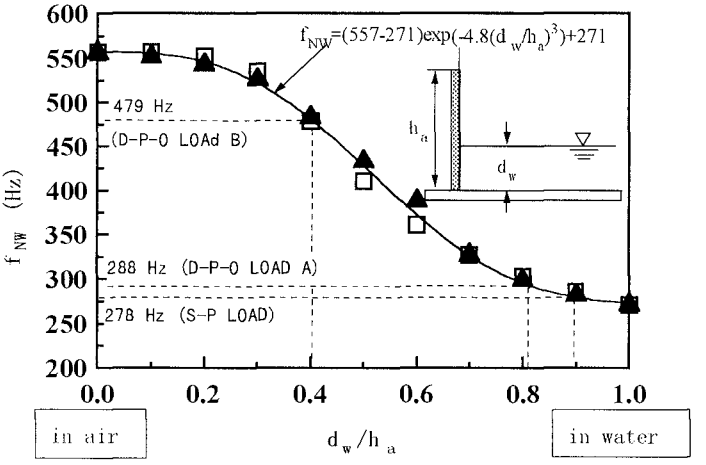

Fig. 3 Natural frequency of the spring metal wall. (1.0 mm-thick)

When pressure transducers are installed on the elastic wall, the output signals are usually contaminated by wall oscillations (Hattori, 1994). To avoid such undesirable effect, eight semi-conductor type transducers (10 mm ϕ , and natural frequency: 3 KHz) were deployed on the rigid wall (Fig. 2). Impact pressures were recorded on digital recorders over six wave periods at a sampling frequency of 5 KHz. The time history of the wave force per unit wall width, $F^*(t)[=F(t)/\gamma H_B^2]$, was computed by depth integration of the pressure time histories. γ is the specific weight of water, and H_B is the breaking wave height.

Wall oscillations excited by wave impact were detected by an accelerometer (natural frequency: 3 KHz) setting up at the elastic wall center(Fig. 2). Using time series data of the wall oscillations, the wall deflection at the wall center $\delta(t)$ was computed by means of a step by step integration of a linear acceleration method.

Experimental Results and Discussions

The wall deflection response depends closely on the magnitude and the rise time of impact forces (Hattori, 1994). Accordingly, we classify the wave loading into the three following modes (Hattori et al., 1994), according to the relationship between the wave force oscillation frequency f_{FO} and the natural frequency of W-D system f_{NW}. That is,

(1) Single peaked load (S-P LOAD) with very short duration: $f_{FO} >> f_{NW}$,

(2) Damped pressure oscillation load A (D-P-O LOAD A): $f_{FO} > f_{NW}$, and
(3) Damped pressure oscillation load B (D-P-O LOAD B): $f_{FO} < f_{NW}$.

Time history records of the wave force and the wall oscillations were examined by the aid of a frequency spectral analysis. The time history records taken from a breaking wave collision are transient data that result from short duration nonstationary phenomena with a clearly defined beginning and end. Hence, frequency spectra of these data will be analyzed by means of techniques commonly used for stationary data.

Figure 4 shows a typical experimental result obtained from the S-P LOAD, an extremely high peak pressure of p_P=1030 N/m^2 [$p^*_P(=p_P/\gamma H_B)$=80.1] occurs at just above the still water level(pressure records not shown). Fig. 4 (A) is time history records of the wave force and the wall oscillations of spring metal of 1-mm thick. $t^*[= t/(H_B/C_S)]$=0 on the time axis refers to the time of the peak wave force. C_S(=1500 m/s)is the sound velocity in water. Three video still pictures on the top of Fig. 4 provide a sequential change of impinging wave shape, at three different instants marked by thick arrows on the top of the time history records.

Fig. 4 (B) shows a comparison between the computed frequency spectra of the wave force and the wall oscillation data. From a comparison between time histories of the wave pressures (not shown) and the wave force (Fig. 4 (A)), we find that despite the peak wave pressures produced by S-P LOAD are extremely high magnitude, the maximum wave force does not attain a high magnitude (F_M=1030 N/m), because of narrow region of the high peak pressures and of subtle time gapes between the peak pressures.

Just after impact, the wall starts to oscillate and keeps on oscillating with a natural frequency of the W-D system even after damping down the wave impact. In Fig. 4 (B), no any spectral peak appears on the frequency spectrum of wave force. In contrast with the wave force, on the frequency spectrum of wall oscillations, a distinct spectral peak is found at a frequency of 278 Hz correspond to the natural frequency of W-D system, in which the wall is almost in water (see Fig. 3, d_W/h_a=0.9).

Under D-P-O LOAD A, a thin air pocket is trapped between the wall and breaking wave front at impact, results in the wave force oscillations with higher frequencies than the natural frequency of the W-D system. Owing to short duration time of the wave force, the maximum wave force (F_M=1720 N/m) is larger than that of S-P load (Fig. 4 (A)). Consequently, as seen in Fig. 5 (A), the spring metal wall of 1.0 mm-thick can not response to very rapid changes of the impact force and keeps to oscillate with its own natural frequency, even after the wave force oscillations damp down. The computed frequency spectrum of wave force record indicates a distinct spectral peak at a frequency of 479 Hz, while that of wall oscillation record shows the only peak at a frequency of 288 Hz, corresponds to the natural frequency of W-D system(see Fig. 3, d_W/h_a= 0.81).

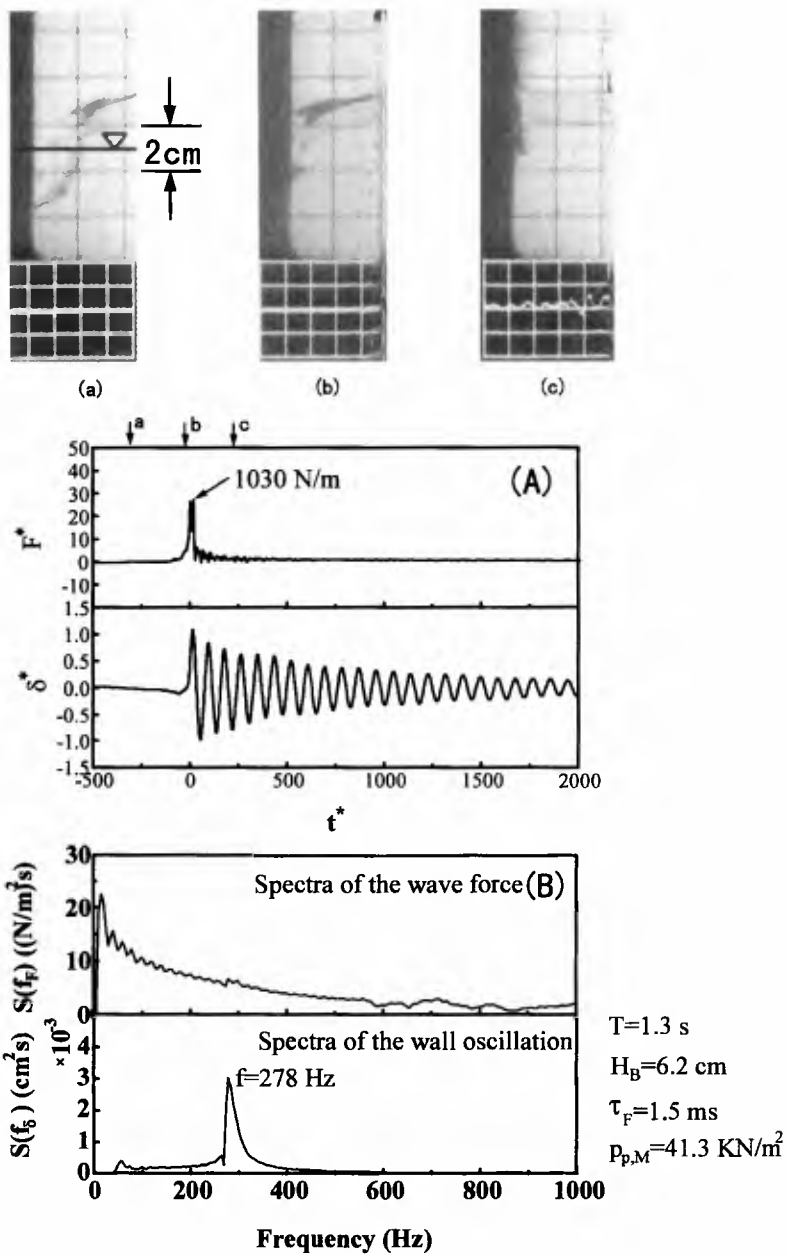

Fig. 4 Time history records of frequency spectra of the wave force and the wall deflection. (S-P LOAD)

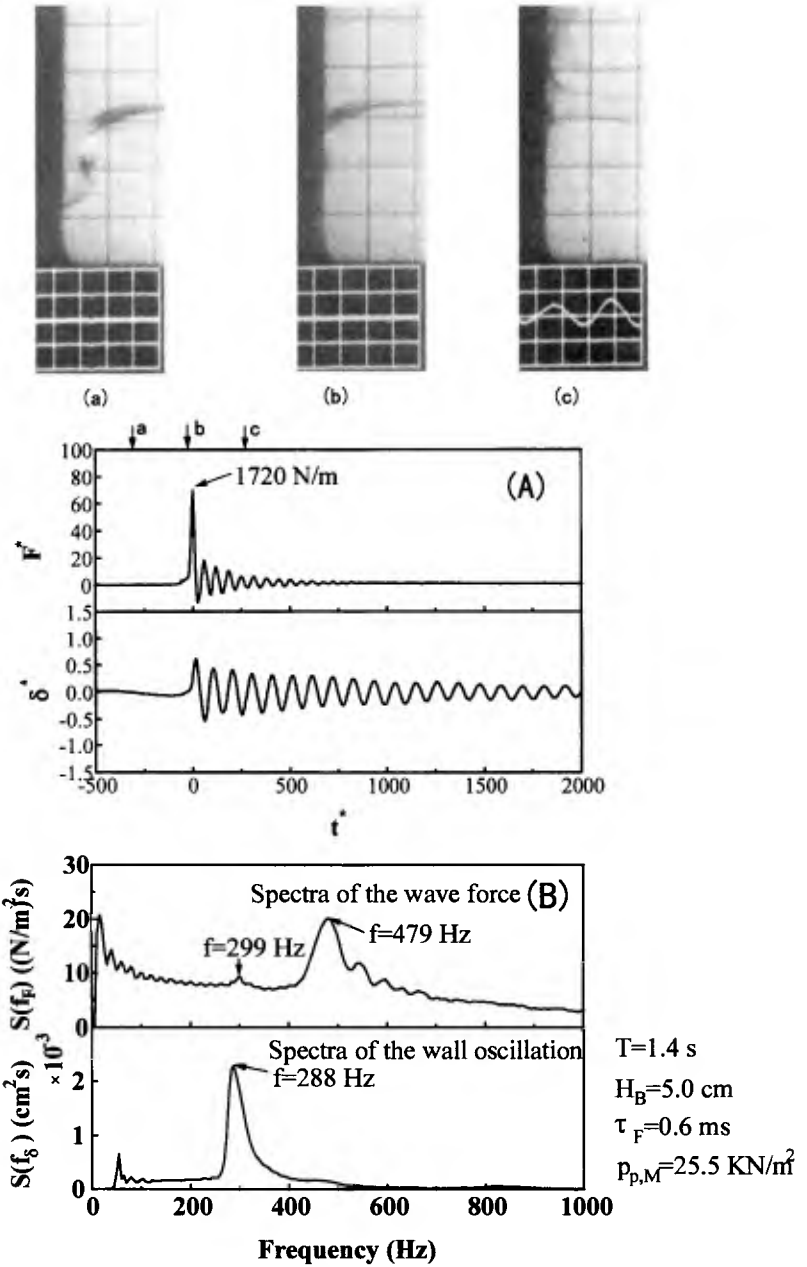

Fig. 5 Time history records and frequency spectra of the wave force and the wall deflection. (D-P-O LOAD A)

Figure 6 shows the time history records taken from D–P–O load B and these computed frequency spectra. The D–P–O LOAD B occurs when a larger air pocket is trapped at impact. Therefore, the peak pressure magnitudes decrease and the pressure rise times increase. These wave loading characteristics are clearly reflected in the wave force record (Fig. 6 (A)). The wave force record also displays a regularly damped oscillations, while the wall oscillation record indicates a rather complicated behavior owing to collisions of irregular wave front of impinging breakers on the wall, as seen in the still pictures on the top of Fig. 6 (A). Frequency spectrum of the wave force record indicates that the wave force oscillates with a frequency of 186 Hz. On the other hand, the wall oscillations are composed of two dominant components in frequency, the natural frequency f_{NW} of 479 Hz (see Fig. 3) and the frequency of 186 Hz, identical with the wave force oscillations. The wall oscillations with 186 Hz frequency attenuate rapidly with the wave force oscillations. It seems that the small spectral peak at 250 Hz indicates the occurrence of the free oscillation of second mode of W–D system.

From the experimental results, we notice the following facts;
(1) When frequencies of the wave force oscillations are higher than the natural frequency of the W–D system (S–P LOAD and D–P–O LOAD A), the only wall oscillation with the natural frequency of W–D system is excited just after the wave impact. On the other hand, D–P–O LOAD B excites wall oscillations with two dominant components in frequency, the wave force oscillation and the natural oscillation of W–D system. In either case, the wall keeps on oscillating with the natural frequency even after the impact force damp down.
(2) The natural frequency of W–D system changes with the contact length of entrapped air pocket with the wall, depends on the wave loading mode (see Fig. 3). Then, the contact length is measured from still video pictures taken at the instant of a wave impact, and the natural frequency of W–D system is estimated by using the pendulum test result. It is found that the natural frequency is almost the same as the measured one.
(3) Wave pressure records taken from the D–P–O LOAD display regular pressure oscillations with almost the same changes in magnitude and in phase (not shown). A thinner air pocket entrapped at impact brings about a higher peak pressure of short duration and results in pressure oscillations with a higher frequency (Hattori et al., 1994). As the result, maxima of the wave force due to D–P–O LOAD tend to be larger than that due to S–P LOAD, which produces very high peak pressures over narrow zone near the still water level. On the basis of the measured pressure record, Figures 7 (a) and (b) show relations of $p^*_{P,M} \sim \tau^*_P$ and $F^*_M \sim \tau^*_F$. $p^*_{P,M}(= p_{P,M}/\gamma H_B)$ is the maximum peak pressure, and $\tau^*_P(=\tau^*_P/(H_B C_S))$ and $\tau^*_F(=\tau_F/(H_B C_S)$ are the rise time of wave pressure and wave force. The variation trend of F^*_M with τ^*_F is similar to that of $p^*_{P,M}$ with τ^*_P. However, we notice that maxima of the wave force due to D–P–O LOAD (open triangles) tends to be greater than that due to S–P LOAD. This is a very important evidence for designing the structure.

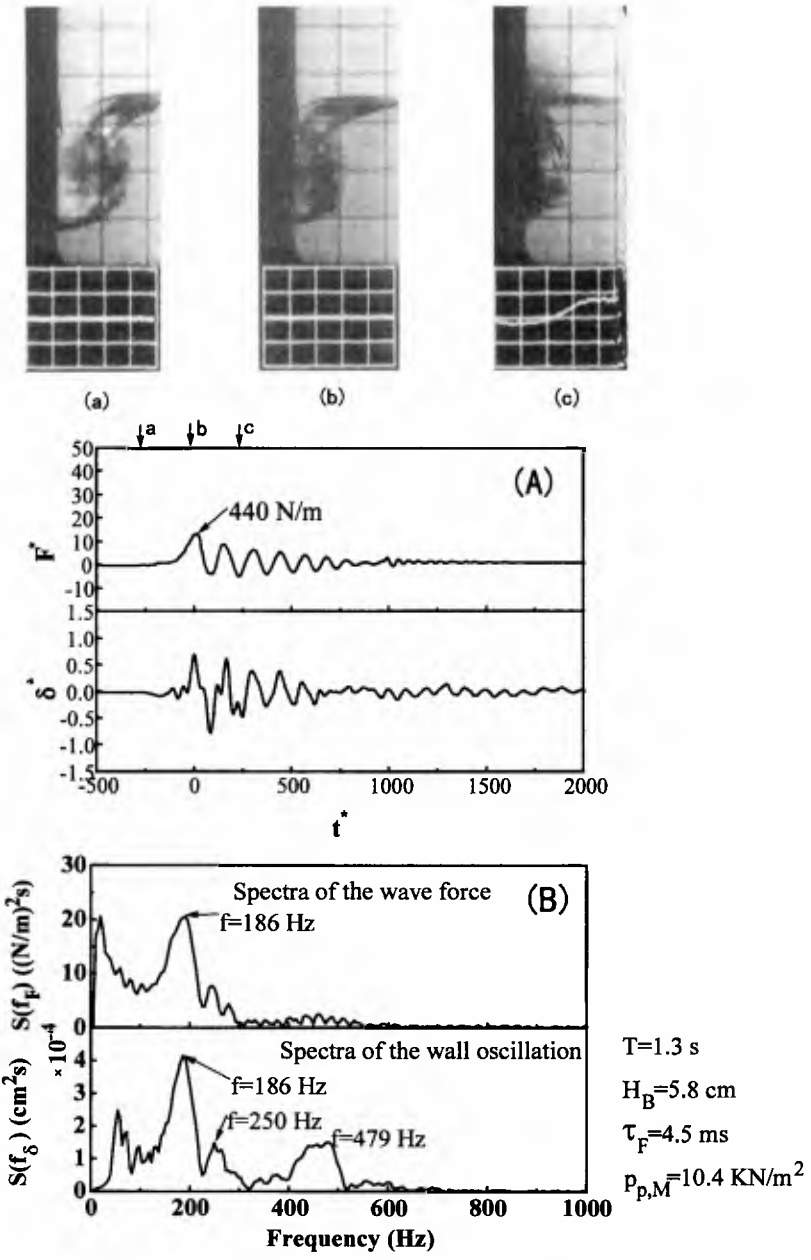

Fig. 6 Time history records and frequency spectra of the wave force and the wall deflection. (D–P–O LOAD B)

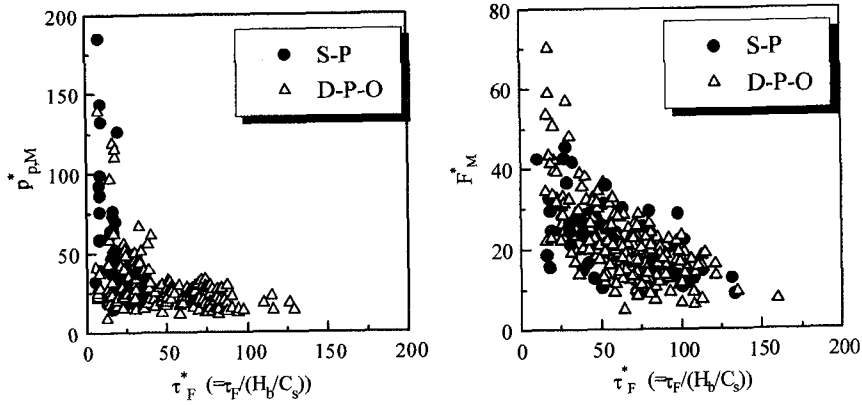

Fig. 7 Relation of $p^*_{P,M} \sim \tau^*_P$ and $F^*_M \sim \tau^*_F$.

(4) As seen in Fig. 4 (A) of the S-P LOAD, the wall oscillations lasting for a long time are gradually damped and maintains a almost constant frequency. This implies that both the fluid damping and the added mass due to the impinging water mass do not practically affect the wall deflection response to a transient impact.

Single Degree-of-Freedom Model for Transient Impact

In the following, we will discuss the wall deflection as a transient phenomenon caused by a wave impact of short duration. Based on the experimental results, assume that any damping and added mass effects caused by the water mass colliding on the wall can be neglected.

We use a single degree-of-freedom model of transient impact, in which the wall at rest is subjected a force input F(t) and produces a wall deflection response δ(t). The equation governing the deflection response of the elastic wall system without damping (Fig. 8) is given by Eq. (1).

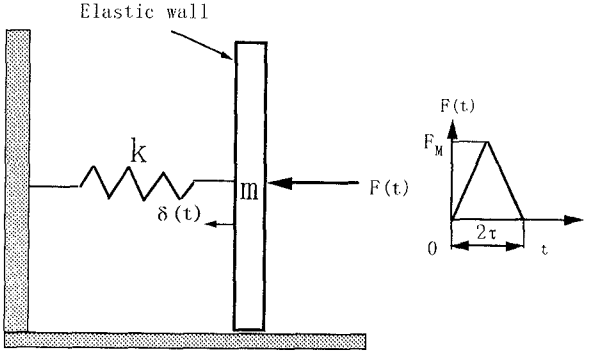

Fig. 8 Wall deflection system for transient impact.

$$m\, d^2\delta(t)/dt^2 + k\delta(t) = F(t)\ , \qquad (1)$$

where m is the wall mass including the virtual mass of impinging water, k is the spring constant, and t is the time. The input force F(t) is assumed by a form of isosceles triangle with the height of F_M and the base of 2τ (Fig. 8). With the initial conditions of

$$\delta = d\delta(t)/dt = 0 : \text{at } t = 0, \qquad (2)$$

the relative wall deflection δ/δ_S is obtained as Eqs. (3) to (5). δ_S is the wall deflection due to the maximum wave force F_M as a static load, distributed uniformly on the wall center elevation.

$$\delta/\delta_S = (t/\tau) - (\sin f_{NW}t/\sin f_{NW}\tau) \quad ; (\,0 \le t \le \tau\,) \qquad (3)$$

$$= (2\tau - t)/\tau + [\,2\sin f_{NW}(t-\tau) - \sin f_{NW}t]/\sin f_{NW}\tau \quad ; (\,\tau \le t \le 2\tau\,) \qquad (4)$$

$$= [2\sin f_{NW}(t-\tau) - \sin f_{NW}t - \sin f_{NW}(t-2\tau)]/\sin f_{NW}\tau \quad ; (\,2\tau \le t\,) \qquad (5)$$

, in which $f_{NW} = (1/2)(k/m)^{1/2}$: the natural frequency of the wall system. From Eqs. (3) to (5), we calculate the gain factor of wall deflection, $\delta^*_M(=\delta_M/\delta_S)$ and the relative lag time $\Delta t^*_\delta(=\Delta t \cdot f_{NW})$ between the maximum force F^*_M and peak deflection δ^*_M (Fig. 9), as a function of the relative rise time $\tau^*_F(=\tau_F \cdot f_{NW})$.

Variations of the gain factor δ^*_M and the lag time Δt^*_δ in terms of τ^*_F are shown in Fig. 9. The single degree-of-freedom model indicates that the largest peak wall deflection due to a given wave force attains 1.5 times as much as the static wall deflection, when the relative rise time $\tau^*_F = 0.45$, and that the peak wall deflection always appears after occurrence of the maximum wave force.

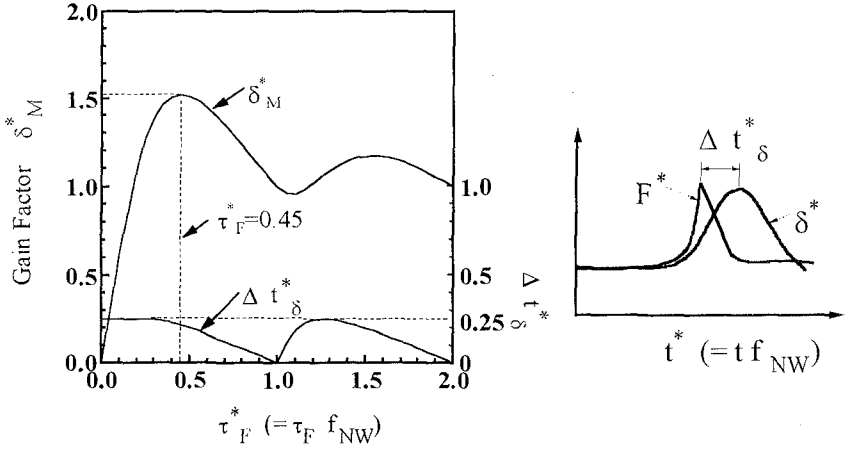

Fig. 9 Variations of δ^*_M and Δt^*_δ.

Figures 10 and 11 show respectively a comparison between the measured and predicted gain factor for 1 mm-thick spring plate and 0.5 mm-thick PVC plate walls.

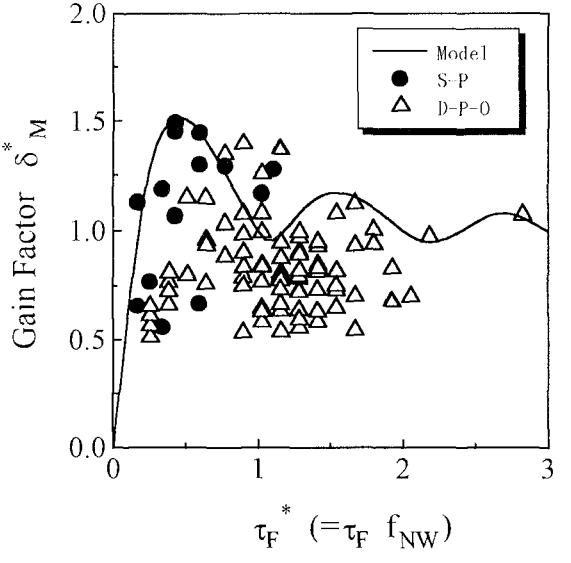

Fig. 10 Gain factor of the wall deflection.
(1.0 mm-thick spring plate wall)

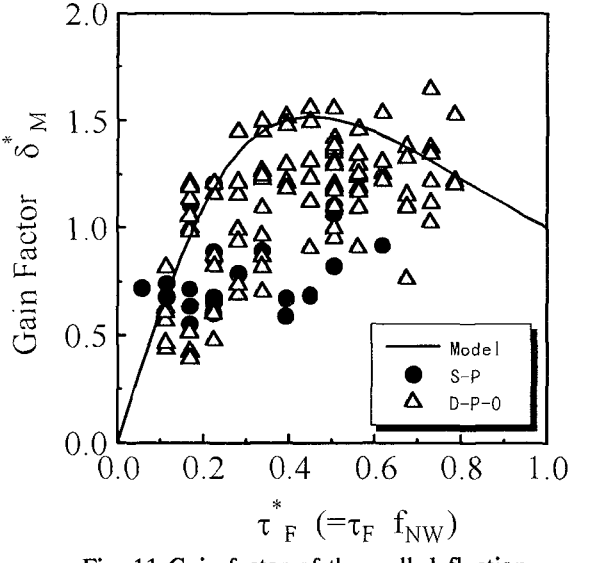

Fig. 11 Gain factor of the wall deflection.
(0.5 mm-thick PVC plate wall)

The solid line represents the model prediction. Although the experimental points are widely scattered owing to variability of the impact processes, the model agrees reasonably well with upper bounds of the experimental points. In case of the spring metal wall (f_{NW}=557 Hz in air), the large gain factor within range of $0 \leq \tau \leq 1$ is produced by the S-P LOAD (solid circles). On the other hand, in case of PVC plate (f_{NW}=300 Hz in air), the large gain factor within the same range appears under the D-P-O LOAD condition (open triangles).

Due to the three-dimensionality of the wave impact process, the convergent crest of breaking waves does not always hit simultaneously the rigid and elastic walls. As the result, we could not obtain reasonably good results on the variation of the delay time Δt^*_δ with the relative rise time τ^*_F.

Conclusions

We conducted laboratory experiments focused on wall deflection responses of the wall member of upright structures to impulsive wave forces. The wall deflection response relates closely not only to the wave load mode, the magnitude and the rise time of impact forces, but also to the natural frequency of the wall deflection system. The single degree-of freedom model of transient impact describe well the wall deflection process. In addition, the experiments point out an very important fact that the wave force produced by single-peaked load is lower than that by the damped-pressure-oscillation load, such as D-P-O LOAD A. The main findings are as follows;

(1) Both S-P LOAD and D-P-O LOAD A, $f_{FO} >> f_{NW}$ and $f_{FO} > f_{NW}$, excite the wall oscillations only with the natural frequency of the W-D system. Such wall oscillations continue for a long time even after the wave impact damp down.

(2) The wall oscillations due to the D-P-O LOAD B, $f_{FO} < f_{NW}$, consist of the two components in frequency, correspond to the wave force oscillations and the natural oscillations of W-D system.

(3) The single degree-of-freedom model of transient impact describes well the wall deflection response and is verified by comparisons of the experiments. The gain factor of the wall oscillation δ^*_M is a function of the relative rise time τ^*_F, and the peak value of δ^*_M attains 1.5, when τ^*_F= 0.45.

References

Hattori, M.(1994): Wave impact pressures on vertical walls and the resulting wall deflections, Proc. of International Workshop on Wave Barriers in Deepwaters, Port and Harbour Research Institute, pp. 332-346.

Hattori, M., A. Arami, and T. Yui(1994): Wave impact pressures on vertical walls

under breaking waves of various types, Coastal Engineering, Elsevier, pp. 79–114.

Kirkgöz, M.S.(1990): An experimental investigation of a vertical wall response to breaking wave impact, Ocean Engineering, Vol. 17, No. 4, pp. 379–391.

Mogridge, G.R. and W.W. Jamieson(1980): Wave impact pressures, ASCE, Proc. 10th Int. Conf. on Coastal Engineering, pp. 1829–1848.

Weggel, J.R. and W.H. Maxwell(1970): Numerical model for wave pressure distributions, Proc., ASCE. Jour. Waterways, Harbors and Coastal Engineering Div., No. WW3, pp. 623–641.

Witte, H.H.(1988): Wave–induced impact loading in deterministic and stochastic reflection, Mitteilungen, Leichtweiss Institut für Wasserbau, Tech. University Braunschweig, 102, pp. 1–227.